Model-Data Comparison of Neutral Wind Impacts on High-Latitude Ionospheric Upflows

M. Burleigh[1], M. Zettergren[1,2], C. Heale[1], and J. Snively[1]

[1]Embry-Riddle Aeronautical University, [2]Boston University

Poster ID: MITC-01

1. Introduction – High-Latitude Ion Upflow

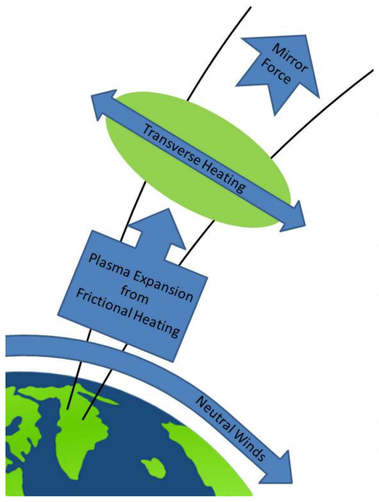

Ionospheric plasma is transported to high altitudes (ion upflow) in response to a variety of plasma heating and uplifting processes. Two common upflow drivers are DC electric fields and soft electron precipitation. Strong DC electric fields can frictionally heat the ion population resulting in anisotropic increases in ion temperature that cause large pressure gradients which push the ions outward and upward. Soft electron precipitation heats F-region electrons creating electron pressure gradients which increase the ambipolar electric field, driving ion upflows. Ions may undergo further acceleration at higher altitudes from transverse heating by broadband ELF waves and at high altitudes, the mirror force can propel ions to escape velocities, resulting in outflow to the magnetosphere.

What role does the neutral wind play in regulating these ionospheric dynamics and ion upflow/outflow? Neutral winds arise from solar forcing, plasma convection, gravity waves, etc. and may interact with ionospheric plasma, through collisions, modulating upflow or perpendicular motion.

2. Gravity waves are in the data…

Sondrestrom incoherent scatter radar (ISR) data from May 31st 2003, from 0:10-8:00 UT, (electron density (panel a), ion temperature (panel b), electron temperature (panel c), and line-of-sight velocity (panel d)) contains velocity perturbations that are uncorrelated with activity in the other panels. The alternating upward/downward flow and downward phase progression suggests the presence of a gravity wave.

Low altitude electron density increase and high altitude (>400 km) upflow from soft electron precipitation

Brief ion temperature increases from frictional heating

Alternating upflow-downflow, and a downward phase progression, at low altitudes (<300km) without a one-to-one correspondence with ion or electron heating suggests the presence of a gravity wave

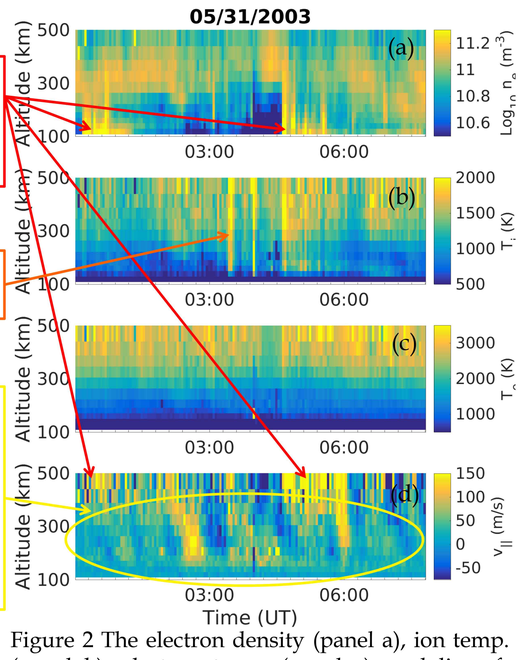

Figure 2 The electron density (panel a), ion temp. (panel b), electron temp. (panel c), and line-of-sight velocity (panel d) from Sondrestrom's ISR.

3. Modeling Neutral Wind Forcing of Ions

Using a pair of coupled models, the ionospheric response to neutral winds, specifically gravity waves, has been simulated. The ionosphere is represented by the 2D anisotropic fluid ionospheric model, GEMINI-TIA, which is based on a truncated 16-moment description, solving the time-dependent, nonlinear equations of conservation of mass, momentum, parallel and perpendicular energy [Burleigh and Zettergren, 2016] for six ion species:

$$\frac{\partial \rho_s}{\partial t} + \nabla \cdot (\rho_s \mathbf{u}_s) = m_s P_s - L_s \rho_s$$

$$\frac{\partial \rho_s \mathbf{u}_s}{\partial t} \cdot \hat{\mathbf{e}}_\parallel + [\nabla \cdot (\rho_s \mathbf{u}_s \mathbf{u}_s)] \cdot \hat{\mathbf{e}}_\parallel = (\rho_s \mathbf{g}) \cdot \hat{\mathbf{e}}_\parallel - \nabla_\parallel p_{s,\parallel} + \left(\frac{\rho_s}{m_s} q_s \boldsymbol{E}\right) \cdot \hat{\mathbf{e}}_\parallel - (p_{s,\parallel} - p_{s,\perp}) \nabla \cdot \hat{\mathbf{e}}_\parallel + \frac{\delta M_s}{\delta t}$$

$$\frac{\partial p_{s,\parallel}}{\partial t} + \nabla \cdot (p_{s,\parallel} \mathbf{u}_s) = -2 p_{s,\parallel} (\nabla_\parallel \cdot \mathbf{u}_s) - \nabla \cdot (h_{s,\parallel} \hat{\mathbf{e}}_\parallel) + 2 h_{s,\perp} (\nabla \cdot \hat{\mathbf{e}}_\parallel) + \frac{\delta E_{s,\parallel}}{\delta t}$$

$$\frac{\partial p_{s,\perp}}{\partial t} + \nabla \cdot (p_{s,\perp} \mathbf{u}_s) = - p_{s,\perp} (\nabla_\perp \cdot \mathbf{u}_s) + \dot{W}_{s,\perp} - \nabla \cdot (h_{s,\perp} \hat{\mathbf{e}}_\parallel) - h_{s,\perp} (\nabla \cdot \hat{\mathbf{e}}_\parallel) + \frac{\delta E_{s,\perp}}{\delta t}$$

The atmosphere is represented by the neutral dynamics model of Snively and Pasko [2008] in the form outlined by Zettergren and Snively [2015] and solves the time-dependent equations of conservation of mass, momentum, and energy:

$$\frac{\partial \rho}{\partial t} + \nabla \cdot (\rho \mathbf{u}) = 0$$

$$\frac{\partial (\rho \mathbf{u})}{\partial t} + \nabla \cdot (\rho \mathbf{u}\mathbf{u} + p\mathbf{I}) = \rho \mathbf{g} + \nabla \cdot \boldsymbol{\tau}$$

$$\frac{\partial E}{\partial t} + \nabla \cdot \big((E + \rho)\mathbf{u}\big) = \rho \mathbf{g} \cdot \mathbf{u} + (\boldsymbol{\nabla} \cdot \boldsymbol{\tau}) \cdot \mathbf{u} + \kappa \nabla^2 T$$

These models are coupled one-way with the neutral wave dynamics calculated first and input into the ionospheric model. The neutral perturbations interact with the ions through ion-neutral collisions and the dynamo source term (equations not shown here).

M. Burleigh was supported by NSF CAREER grant AGS-1255181. M. Zettergren was supported by NASA grant NNX15AJ08G and NSF CAREER grant AGS-1255181.

4.1. Modeled Ionospheric Response to Simple Gravity Waves

In order to produce conditions similar to those observed in the May 2003 event (see section 2) a gravity wave is excited in the neutral atmosphere model by vertical forcing at ~110 km with a period of 78 minutes. The forcing amplitude is ramped up slowly over 117 minutes to avoid wave breaking and then held steady until the simulation end. The neutral atmosphere model's density, temperature, and velocity perturbations are used as inputs into the anisotropic ionospheric model. The ion response is shown in Figures 4.1.1 and 4.1.2 (right)

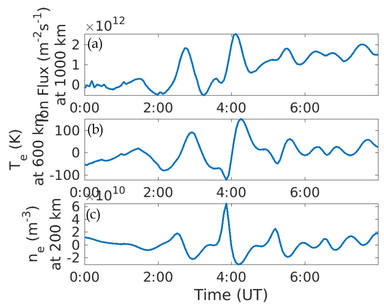

Figure 4.1.3 The ion flux (panel a), detrended electron temperature (panel b), and detrended electron density (panel c) at different altitudes highlighting the connections driving upflow.

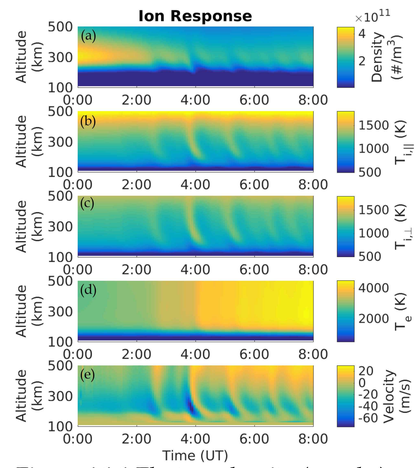

Figure 4.1.1 Electron density (panel a), ion parallel temp. (panel b), ion perp. temp. (panel c), electron temp. (panel d), and field aligned velocity (panel 3) response to a simple gravity wave.

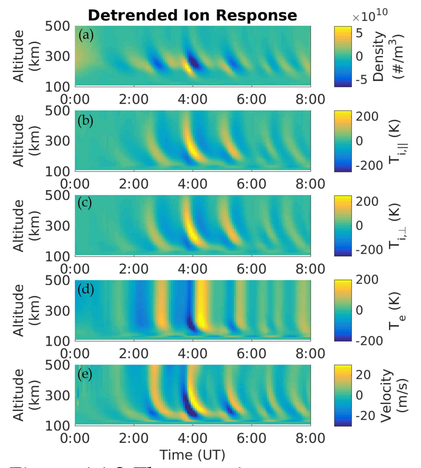

Figure 4.1.2 The same ion parameters as shown in Figure 4.1.1 detrended using a moving average to remove the background trends and highlight the gravity wave forcing effects.

As the gravity wave forcing continues over time, the neutral atmosphere is dragging the ionosphere around modulating the ion density (altitude specific example in Figure 4.1.3, panel c). This density modulation alters the electron temperature response to photoionization (panel b). These electron temperature modulations rapidly conduct upwards along the field lines increasing the ambipolar electric field driving ion upflow in the topside (panel a).

4.2. Modeled Ionospheric Response to Strong Gravity Waves

The simple gravity wave simulation, section 4.1 above, results in an ion velocity response smaller than that observed in the May 2003 event. Increasing the amplitude of the gravity wave increases the ionospheric upflow response but also results in wave breaking. The forcing altitude has been lowered to ~88km. Within this simulation of strong gravity wave forcing the same ionospheric responses drive upflow even with the complications from nonlinear wave effects and wave breaking.

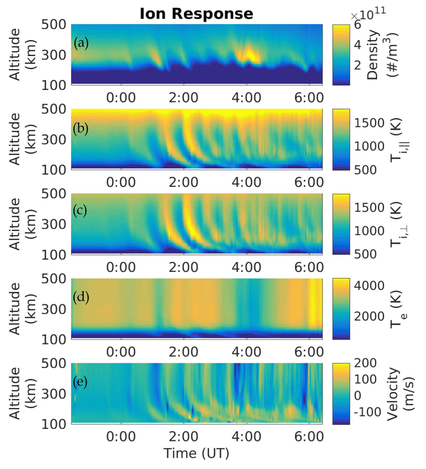

Figure 4.2.1 The electron density (panel a), ion parallel temp. (panel b), ion perp. temp. (panel c), electron temp. (panel d), and field aligned velocity (panel e) from a strong gravity wave simulation.

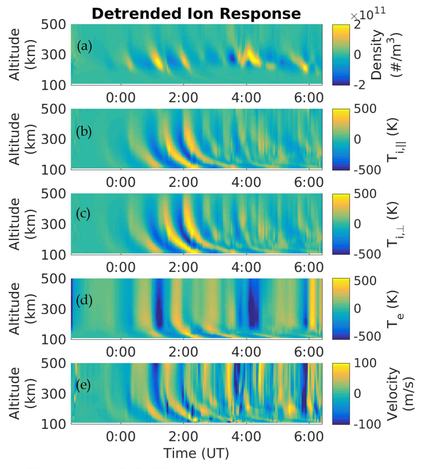

Figure 4.2.2 The same parameters as shown in Figure 4.2.1 also detrended with a moving average to remove the daily cycle background and highlight the gravity wave forcing effects

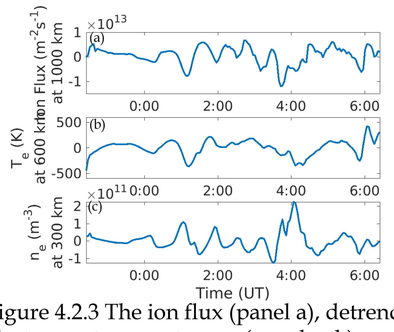

Figure 4.2.3 The ion flux (panel a), detrended electron temperature (panel b), and detrended electron density (panel c) at different altitudes highlighting connected responses responsible for upflow.

5. Conclusions and Future Work

What is the role of neutral wind disturbances in regulating ion upflow? The primary upflow response in the simulations is due to gravity wave modulation of the ion density. This density variation impacts the electron temperature heating response to photoionization (since this is summer – there is still photoionization at these UT). The heated electrons undergo thermal expansion (and upflow) which, through the ambipolar electric field, drive ion upflow.

Do the simulations represent the base processes driving upflow in the ISR data? The ISR data is highly variable, similar to the strong gravity wave case (section 4.2), does not show the chain of process responsible for driving upflow as clearly, see data plotted in Figure 5.1 below, and the source of the gravity wave is unknown. In an effort to elucidate more information about the gravity wave seen in the ISR data, the wavelet analysis from Torrence and Compo (1998) is used. The resulting wavelet power spectrum of the field aligned velocity at an altitude of 300 km from the ISR data (bottom), simple gravity wave (top), and strong gravity wave (center) cases are shown in Figure 5.2. The spectrum from the simple gravity wave case retains both a primary wave mode and a single harmonic. The strong gravity wave case's spectrum starts out with the primary wave mode, which is destroyed due to wave breaking, resulting in the wave mode that contains the most power transitioning to shorter periods over time. The ISR data's wavelet power spectrum also shows evidence of a complicated, high power, gravity wave situation with nonlinear wave effects and wave breaking. We are presently examining higher resolution data from the ISR event looking for direct evidence of wave breaking which would increase confidence in the presence of stronger wave inputs than those used in the strong gravity wave case.

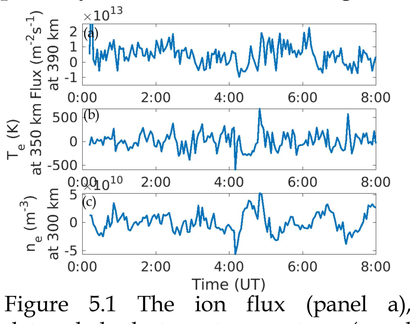

Figure 5.1 The ion flux (panel a), detrended electron temperature (panel b), and detrended electron density (panel c) at different altitudes. The connection between processes is not as straightforward within this dataset. The temporal resolution prohibits the direct detection of the signatures of wave.

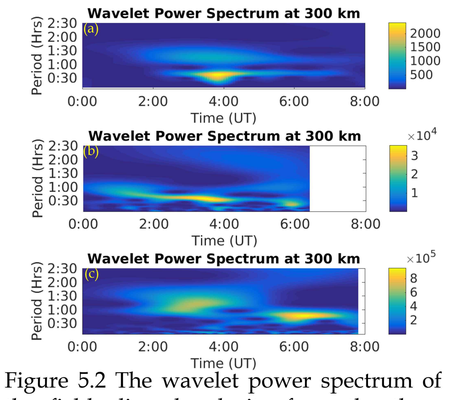

Figure 5.2 The wavelet power spectrum of the field aligned velocity from the three cases discussed here: a) simple gravity wave forcing, b) strong gravity wave forcing, c) Sondrestrom ISR data, all taken at 300 km.